THE ORIGIN OF LUNAR CONCENTRIC CRATERS. D. Trang[1], J. J. Gillis-Davis[1], B. R. Hawke[1], and D. B. J., Bussey[2], [1]Hawaii Institute of Geophysics and Planetology, University of Hawai'i at Mānoa, 1680 East-West Rd. POST517, Honolulu, HI 96822 (dtrang@higp.hawaii.edu). [2]Applied Physics Laboratory, Laurel, MD 20723.

Introduction: Lunar simple craters are typically bowl-shaped with diameters <20-km [1,2]. However, a class of craters, in the same size range but contain a torus-shaped scarp in the interior of the bowl are referred to as concentric craters [3]. Interpretations for the origin of concentric craters and their inner torus include exogenic processes (e.g., simultaneous impacts [4], impact into layered targets [5]) as well as endogenic ones (e.g., mass wasting [6], volcanic extrusion [3,6,7], and igneous intrusion [5]). Before now, consensus for their formation had not been established. Hence, the purpose of this study is to understand the formation of concentric craters by comparing the morphology of multiple lunar and terrestrial landforms with concentric craters in order to infer the most probable mechanism of formation for these craters. To this end, we integrated data from Clementine, SELENE and the Lunar Reconnaissance Orbiter (LRO) to better comprehend the form, structure, composition and distribution of these craters. Depending on their mechanism of formation, study of these craters could provide insight on an impactor population unique to Earth-Moon space because they are unique to the Moon, or additional information about the Moon's thermal history.

Data Sets: We used Clementine, SELENE, and the data from two instruments on LRO: Miniature-Radio Frequency (Mini-RF), and Lunar Orbiter Laser Altimeter (LOLA). An initial global survey for concentric craters was completed through examining both Clementine images and Mini-RF radar data. In addition, we produced FeO and optical maturity (OMAT) maps with the Clementine UVVIS data set [8,9]. Next, the SELENE Multispectral Imager (MI) provided 20-m/pixel resolution [10] for measuring crater and torus diameter. Crater rim height, rim-width flank, torus height, and crater depth were measured with LOLA.

Concentric Craters: Currently, there are 58 known concentric craters including 44 craters from [3] and 14 additional craters detected in this study. The 58 concentric craters have diameters ranging from 3-20-km, with a median ~8-km in diameter.

Morphometrics: We identified three types of concentric craters (Fig. 1), which represent end-members instead of separate types. The first end-member consists of a continuous smooth inner torus. The join between the crater wall and the torus is a V-shaped valley. Another end-member has a 'ring of hills' situated in the crater. The third end-member is composed of a continuous torus except the join between the crater wall and the torus is an inflection point. Some concentric craters contain a combination of these different end-members.

To understand how concentric craters were modified, we compared them to fresh simple craters. As investigated by many authors [e.g., 1,2], fresh simple crater parameters like, rim height, rim-flank width, crater depth tend to be intimately related to crater diameter. For example, the crater depth to diameter ratio is about 1:5 for fresh lunar craters [1,2]. We compared these different parameters to those of concentric craters and found that concentric craters have shallower depths, shorter rim-flank widths, and smaller rim heights, which suggests concentric craters experienced degradation from impact degradation and/or a combination of other mechanisms like uplift of the crater floor.

Distribution: Concentric craters are typically located near mare/highland boundaries [3], in the vicinity of isolated mare ponds, and within floor-fractured craters. Floor-fractured craters have had their floors modified due to uplift from igneous intrusions [11]. Furthermore, the distribution of floor-fractured craters and concentric craters is similar.

Composition: FeO maps were derived from Clementine's UVVIS using a method developed by [8]. The FeO content of the interior of concentric craters differs by 1 wt% to the surrounding area. However, there are three concentric craters with FeO content 2-6 wt.% lower than the local area.

Age: We examined the age of 22 concentric craters based on USGS maps of the Moon. Of these 22 concentric craters, 2 have been assigned Pre-Imbrian (>3.85-Ga), 15 Imbrian (3.2-3.85-Ga), and 5 Eratosthenian (1.1-3.2-Ga).

Discussion: The mechanism responsible for the formation of concentric craters could be endogenic or exogenic. In order to determine the most plausible origin, we compared the morphology, spatial distribution, composition and age predicted by each mechanism to the observed data for concentric craters.

Exogenic: Peak-ring basins are impact related features. They are 175-440-km in diameter with an inner ring [12]. They are distributed globally and are more exclusively found on highlands terrain. From the size and spatial distribution, they do not match the observation of concentric craters. Thus, the formation of peak-ring basins is probably not similar to the formation of concentric craters.

It was proposed that concentric craters are a product of two simultaneous impacts over the same position [4]. If concentric craters are a result of dual impacts, then

they should exist randomly and more frequently on older surfaces. This spatial distribution is not observed for concentric craters.

In addition to concentric craters, there are also sub-kilometer concentric craters. Sub-km concentric craters are a result of an impact into a weaker layer over a stronger substrate [13]. Since the morphology of these craters is dependent on layering of the target, it is expected that craters in the vicinity of a concentric crater, and of similar size, would also have a concentric geometry [14]. This grouping of concentric craters is rarely the case for concentric craters.

Endogenic: Mass wasting from crater walls is commonly observed as scallops or terraces. Scallop appears as sheet-like masses [15] and terraces are block slumps from the crater wall [16]. Craters with these two textures are spatially distributed on highlands and maria. Furthermore, the craters with wall failure ranges from Pre-Imbrian to Copernican – There are no Copernican concentric craters. Consequently, mass wasting is not the probable mechanism in producing the inner torus.

Extrusive domes were suggested for the origin of concentric craters [7]. Such domes were constructed by two cycles of lava extrusion followed by a cratering event in the center of the dome [7]. To confirm whether an extrusion occurred in concentric craters, we examined Clementine derived FeO maps. We observed no compositional differences between the interior of concentric craters and the surrounding area. This observation suggests mafic extrusion is not a likely scenario.

Viscous relaxation involves the decrease of viscosity with depth. As a result long-wavelength topography is modified [17]. The effects of viscous relaxation were tested on craters of all sizes. Models found that relaxation of even small craters would hardly be affected even at timescales of the Solar System [17]. Therefore, viscous relaxation is not considered a viable mechanism.

Floor-fractured craters are a type of landform that developed due to igneous intrusions [11]. In fact, floor fractures size ranges from simple craters to peak-ring basins [11]. Also, the spatial and temporal distributions of floor-fracture craters are nearly identical to concentric craters. Floor-fractured craters differ from concentric craters morphologically, as most floor-fractured craters do not contain an inner ring. The lack of compositional differences between concentric craters and the surrounding area also enhances the case for igneous intrusion. Accordingly, igneous intrusions are the most likely candidate in forming concentric craters.

Conclusion: We examined seven possible mechanisms to understand the origin of concentric craters. An exogenic origin does not easily explain the formation of the inner torus and why concentric craters are focused along highland/mare boundaries. The distribution argument is also true for a mass wasting mechanism, sub-km craters, peak-ring craters and multiple impacts. In addition, we do not see compositional variations between the crater and the surrounding area, making extrusion unlikely. Also, the role of viscous relaxation is negligible. On this basis, the mechanism we find most probable is modification by igneous intrusion.

References: [1] Pike R.J. (1980) *USGS Prof. Paper*, 1046-C, C1-C77. [2] Wood C.A. and Andersson L. (1978), *Proc. Lunar Sci. Conf 9th*, 3669-3689. [3] Wood C.A. (1978) *LPS IX*, 1264-1266. [4] Sekiguchi N. (1970) *The Moon*, 1, 429-439. [5] Wöhler C. and Lena R. (2009) *LPS XL* Abstract #1091. [6] Schultz P.H. (1976) *Moon Morphology*. [7] Smith E.I. (1973) *The Moon*, 6, 3-31. [8] Lucey P.G. et al. (2000) *JGR*, 105(E8), 20,297-20,305. [9] Lucey P.G. et al. (2000) *JGR*, 105(E8), 20,377-20,386. [10] Ohtake M. et al. (2008) *Earth Planets Space*, 60, 257-264. [11] Schultz P.H. (1976) *The Moon*, 15, 241-273. [12] Head J.W. (1978) *LPS IX*, 485-487. [13] Quaide W.L and Oberbeck V.R. (1968) *JGR*, 73(16), 5247-5270. [14] Oberbeck V.R. *Personal Comm.* [15] Cintala M.J. et al. (1977) *Proc. Lunar Sci. Conf. 8th*, 3409-3425. [16] Settle M. and Head J.W. (1979) *JGR*, 84(B6), 3409-3425. [17] Dombard A.J and Gillis J.J. (2001) *JGR*, 106(E11), 27,901-27,909.

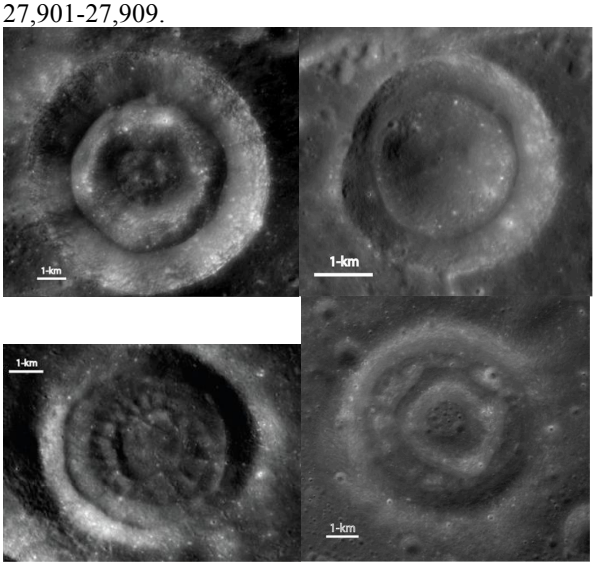

Figure 1 – Top left figure reveals a concentric crater with a V-shaped valley between the crater wall and the inner torus. The top right figure illustrates the inflection point morphology at the join of the torus and the crater wall. Bottom left figure shows multiple ring of hills. Bottom right figure demonstrates a concentric crater with both ring of hills and V-shaped valley morphologies. The scale in each figure is 1-km.